CHAPTER I:

The Neutron Spin Echo Method

THE PRINCIPLES OF NEUTRON SPIN ECHO

F. MEZEI

Institut Laue-Langevin
156X, 38042 Grenoble Cédex, France

and

Central Research Institute for Physics
H-1525 Budapest 114, P.O.Box 49, Hungary

INTRODUCTION

Neutron Spin Echo (NSE) is a particular experimental technique in inelastic neutron scattering. It is substantially different from the other, the "classical", methods both conceptually and technically. Conventionally, an inelastic neutron scattering experiment consists of two steps, viz. preparation of the incoming monochromatic beam and analysis of the scattered beam. The values of the measured energy and momentum transfer are then determined by taking the appropriate differences between the incoming and outgoing parameters measured in the two above steps. In NSE, both the incoming and outgoing velocity of a neutron (more precisely given components of these) are measured by making use of the Larmor precession of the neutron's spin. This kind of measurement could be called "internal" for each neutron, since the Larmor precession "spin clock" attached to each neutron produces a result stored on each neutron as the position of the spin vector serving like the hand of a clock. This is in contrast to the classical monochromatization or analysis, in which cases neutrons within a given velocity band are singled out "externally", i.e. by a selecting action measuring equipment. This difference is the technical one. In addition, since the Larmor precession information on the incoming velocity (component) of each neutron is stored on the neutron itself, it can be compared with the outgoing velocity (component) of one and the same neutron. Thus in NSE the velocity (component) change of the neutrons can be measured directly, in a single step, which is its conceptual novelty.

In this introductory paper the principles and the different types of applications of NSE are described. Although the presentation is self-contained, most technical and mathematical details are omitted here. These are extensively dealt with in the subsequent contributions and in the original papers reproduced in the Appendix of this volume, and the reader will be provided with ample references to these. In the first section the basic facts about Larmor precession in a polarized beam and the notion of the spin echo action are discussed. The second section is devoted to the introduction of the simplified principle of Neutron Spin Echo as a method of inelastic neutron scattering spectroscopy, applicable to quasi-elastic and non-dispersive inelastic scattering processes. The following section gives the generalization of the NSE principle for the study of dispersive elementary excitations; the

final one describes the effect of sample magnetism introducing the notions of Paramagnetic, Ferromagnetic and Antiferromagnetic NSE.

1. LARMOR PRECESSION AND SPIN ECHO

To the best of my knowledge Larmor precession in a neutron beam traversing a magnetic field region was first observed by Drabkin et al.[1] as early as 1969. Unfortunately this work was not known to me until recently; it was in 1972 that I started to work on Larmor precession by introducing a simple new technique for turning the neutron spin direction in any desired direction with respect to the magnetic field direction[2] (see also the Appendix). This technique is described in the following paper by Otto Schärpf, together with more details about Larmor precessions. For the moment it is sufficient to recall that in a neutron beam travelling through a homogeneous magnetic field H_o and polarized originally parallel to the magnetic field direction $z||H_o$, one can initiate Larmor precession by turning the polarization direction $\vec{P}$ perpendicular to the z axis, say into the x direction at a given point (surface) A along the trajectory (Fig. 1).

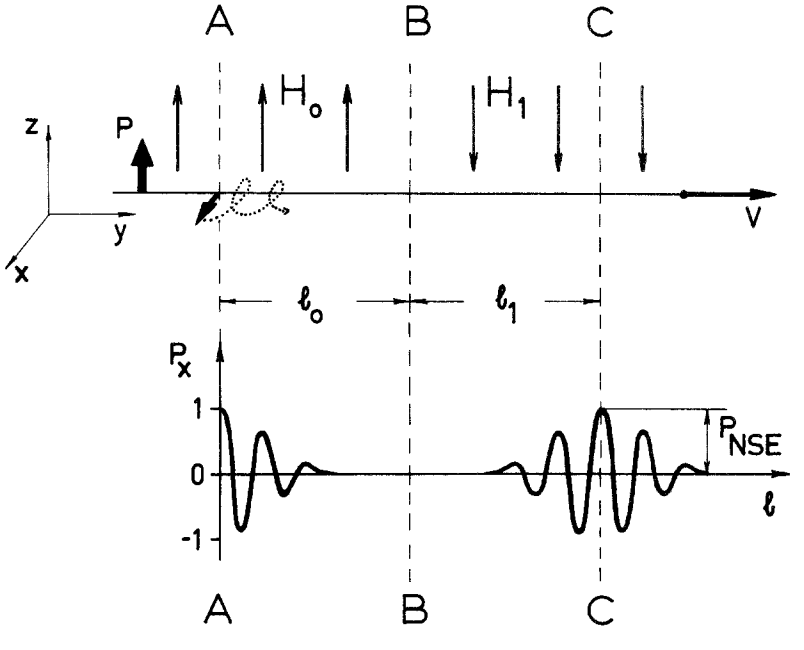

Fig. 1. Larmor spin precession of neutrons in a beam and the simple spin echo effect.

This $\frac{\pi}{2}$ turn initiates the Larmor precession which can be physically characterized, for example, by the x component of the neutron polarization - which obviously has a value of 1 at A. The basic fact about Larmor precessions in spin $\frac{1}{2}$ particle beams is that they can be exactly described classically except in situations where the Stern--Gerlach effect is appreciable, which only happens in very extreme cases with neutrons. This means that the particle beam will be described by a classical velocity distribution function f(v), and for each point-like particle the "classical" spin vector $\vec{S}$ follows the $d\vec{S}/dt=\gamma_L[\vec{S}x\vec{H}]$ classical equation of motion. A rigorous quantum mechanical proof of this theorem has been described recently by the author[3]. Thus the Larmor precession angle φ for a given neutron at a distance ℓ from A (Fig. 1) will be given as

$$\varphi = \gamma_L \frac{\ell H_o}{v} \quad , \tag{1}$$

where γ_L=2.916 kHz/Øe. Since we measure φ with respect to the initial direction x, the polarization component P_x for the beam is given by the beam average

$$P_x = \langle\cos\varphi\rangle = \int f(v)\cos\left(\frac{\gamma_L \ell H_o}{v}\right)dv \tag{2}$$

(Notice that here P_x is given as the Fourier transform of the distribution function for $\frac{1}{v}$, viz. $F(\frac{1}{v})=v^2 f(v)$, which is in fact the wavelength spectrum. This point is discussed in detail in the contribution of John Hayter; and also in the Appendix[4].) The behaviour of P_x with ℓ is easily seen from Eq.(2). As ℓ increases, the differences between φ's for different v's become bigger and bigger, i.e. the Larmor precessions for different neutrons become more and more out of phase. Consequently, the average $\langle\cos\varphi\rangle$ will tend to zero, and we obtain the characteristic behaviour of P_x shown in the lower part of Fig. 1 between A and B; this behaviour was observed by Drabkin et al. in 1969. The period of the damped oscillation is obviously related to the average beam velocity. Thus the observation of Larmor precessions is a simple way of measuring neutron velocities though it tends to be somewhat over-sensitive except for special high precision problems such as the one described by W. Weirauch et al. later in this volume. This sensitivity is illustrated by the large value of φ=1832 rad for H_o=100 Øe, ℓ=1 m and v=1000 m/sec (λ=4 Å).

In order to make more general use of the high sensitivity of Larmor precessions we have to eliminate this dephasing effect arising from the velocity distribution f(v). This is where the echo principle, common to various physical phenomena (one of which is described in the contribution of Badurek, Rauch and Zeilinger), becomes instrumental. In the present case it is realized by making the neutrons precess in the opposite sense after a certain time. This happens in section BC in Fig. 1, where field H_1 is opposite H_o. At point C

$$\varphi = \varphi_{AB} - \varphi_{BC} = \gamma_L (H_o \ell_o - H_1 \ell_1)/v \qquad (3)$$

and if the configuration is "symmetric", that is, $H_o \ell_o = H_1 \ell_1$, φ will be zero for all velocities v and thus $P_x = \langle \cos\varphi \rangle = 1$. Obviously, as is also illustrated in Fig. 1, P_x will show the same damped oscillation behaviour on both sides of C as that described for point A, since differences in φ build up in exactly the same way on moving away from C. It is clear from Eq.(3) that only the difference $H_o \ell_o - H_1 \ell_1$ is important, and in view of this the number of both the forward and the backward precessions, φ_{AB} and φ_{BC}, respectively, can be arbitrarily big (assuming that the fields H_o and H_1 are sufficiently stable and homogeneous). We will call this behaviour of the polarization P_x a "spin echo group" and the amplitude of the P_x oscillation at the symmetry position C will be called "spin echo signal", P_{NSE}. As has been pointed out, the spin echo group is the Fourier transform of the $\frac{1}{v}$ distribution function, $v^2 f(v)$, thus the narrower this distribution, the more oscillations are contained in the group, as shown by the measured curves in Fig. 2. Note that in practice one would change H_1 rather than ℓ_1; furthermore, H_o and H_1 will be parallel and the neutron spins are flipped at B instead, as in NMR spin echo (cf. Otto Schärpf's paper for details).

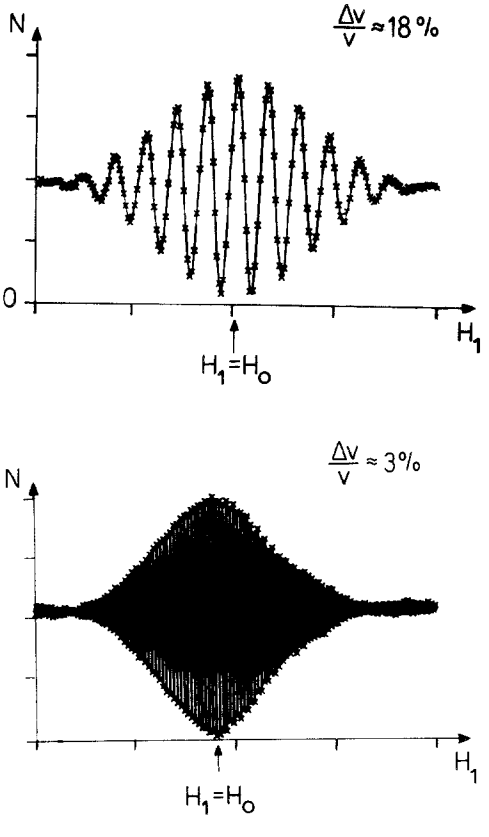

Fig. 2. NSE groups measured with two different beam monochromatizations (raw data).

The way P_x can be measured at C consists of applying another $\frac{\pi}{2}$ turn at this point, thus turning P_x into $\pm P_z$ depending on the sense of the $\frac{\pi}{2}$ turn. Then a usual spin analyser placed before the detector allows the determination of P_z by showing a maximum transmission for $P_z=1$ and a minimum for $P_z=-1$. Depending on the sense of the $\frac{\pi}{2}$ turn at C the $P_x=1$ echo maximum will be observed either as a maximum, or as a minimum of the detector counting rate N. (A comparison of these two values is one way of measuring P_{NSE}.) The data in Fig. 2 were obtained by choosing a $P_x \rightarrow P_z$ turn.

For those readers familiar with classical polarized neutron work, there is a general remark to be made here about the calculation of polarization figures in NSE. The usual definition of $P=(N_+-N_-)/(N_++N_-)$ has one inconvenience: it is nonlinear in N_+ and N_-, thus it is not additive for different contributions, and the comparison of different polarization figures for the same beam, e.g. P_x and P_z, becomes tedious too. Since the polarizer and analyser efficiencies are constant for the whole experiment, it is generally more convenient to take the polarization as being just proportional to the modulation: $P=(N_+-N_-)/N_o$, where the constant denominator N_o has been determined in the usual way from just one of the polarization measurements. This gives a linear definition for P, and since polarization figures will only be considered relative to each other (e.g. P_{NSE} with respect to the incoming beam polarization P_o or P_{NSE} signals measured for different samples), the polarization efficiency factors for the different spectrometer components need not be known. For example in Fig. 2 we can define the spin echo signal P_{NSE} as $(N_{max}-N_{min})/2N_{ave}$, where N_{max} and N_{min} correspond to the highest maximum and the lowest minimum of the curve, and N_{ave} is the counting rate outside the spin echo group.

To conclude this section let us remark that the essential physical reason for the appearance of the NSE group is that at C the Larmor precession angle φ is stationary over the beam:

$$\left(\frac{\partial \varphi}{\partial v}\right)_{beam} = 0 \qquad (4)$$

and not that φ is identically zero. The P_x precessing polarization is produced by all neutrons in the beam having the same spin direction φ at a given point, no matter how this common direction comes about. The shape of the NSE group is then determined by the dephasing of the spin precessions "locally", around the echo point, thus it depends only on the f(v) distribution of the detected neutron beam. Equation (4) is thus the echo condition to be used in what follows.

2. SPIN ECHO WITH SCATTERED NEUTRON BEAMS

Let us consider the configuration shown in Fig. 3. This configuration only differs from the previous one by the neutron beam being scattered on a sample between the forward and backward precessions. For simplicity the precessions in the well controlled small field around the sample, between H_o and H_1, are neglected. (In practice

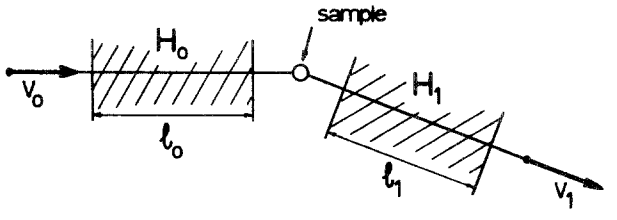

Fig. 3. Application of NSE to inelastic neutron scattering.

these count either for H_o or H_1, the two precession regions being separated by a spin flipper coil, cf. the paper by Otto Schärpf.) The total Larmor precession angle now reads, instead of Eq.(3),

$$\varphi = \varphi_{in} - \varphi_{out} = \gamma_L \left(\frac{\ell_o H_o}{v_o} - \frac{\ell_1 H_1}{v_1} \right) = \varphi(v_o, v_1) \quad , \tag{5}$$

where v_o and v_1 are the incoming and outgoing neutron velocities, respectively. If there is only elastic scattering $v_o = v_1 = v$, in which case the situation is exactly what it was before. In inelastic scattering the neutron energy change is the relevant quantity in which we are interested, viz.

$$\hbar\omega = E_1 - E_o = \tfrac{1}{2} m v_o^2 - \tfrac{1}{2} m v_1^2 = \hbar\omega(v_o, v_1) \quad . \tag{6}$$

The basic idea of NSE inelastic spectroscopy is to use φ as given by Eq.(5) to measure ω. Since $\varphi(v_o, v_1)$ and $\omega(v_o, v_1)$ are different functions, this is only possible locally with respect to an arbitrarily chosen value ω_o. To achieve this, we will use neutron beams such that the average neutron velocities $\bar{v}_o$ and $\bar{v}_1$ correspond to ω_o: $\omega(\bar{v}_o, \bar{v}_1) = \omega_o$. Then we require

$$\varphi - \bar{\varphi} = t(\omega - \omega_o) \tag{7}$$

where $\bar{\varphi} = \varphi(\bar{v}_o, \bar{v}_1)$ and t is a proportionality constant. This is the fundamental equation of NSE spectroscopy. It postulates that locally around "ideal" values given by $\bar{v}_o$, $\bar{v}_1$ the Larmor precession angle φ becomes a measure of the neutron energy transfer ω. Obviously this equation can only be satisfied in first order in $\delta v_o = v_o - \bar{v}_o$ and

$\delta v_1 = v_1 - \bar{v}_1$. Namely, from Eq.(5):

$$\varphi - \bar{\varphi} = -\gamma_L \frac{\ell_o H_o}{\bar{v}_o^2}\delta v_o + \gamma_L \frac{\ell_1 H_1}{\bar{v}_1^2}\delta v_1 \qquad (8)$$

and from Eq.(6)

$$\omega - \bar{\omega}_o = \frac{m}{\hbar} v_1 \delta \bar{v}_1 - \frac{m}{\hbar}\bar{v}_o \delta v_o \quad . \qquad (9)$$

Thus the NSE equation (7) is satisfied if the coefficients of the independent variables δv_o and δv_1 agree on both sides:

$$\gamma_L \ell_o \frac{H_o}{\bar{v}_o^2} = t\frac{m}{\hbar}\bar{v}_o \quad , \qquad \gamma_L \ell_1 \frac{H_1}{\bar{v}_1^2} = t\frac{m}{\hbar}\bar{v}_1 \qquad (10)$$

Since these equations are identical for both indices 0 and 1, in what follows i stands for both. Equations (10) are called the NSE conditions. They can be given in the more practical form

$$\frac{\ell_o H_o}{\ell_1 H_1} = \frac{\bar{v}_o^3}{\bar{v}_1^3} \quad , \qquad t = \frac{\hbar \gamma_L \ell_i H_i}{m\bar{v}_i^3} = \hbar\frac{\bar{\varphi}_i}{2\bar{E}_i} \quad . \qquad (11)$$

Equations (11) are used in practice to choose the ratio of the magnetic fields to obtain the echo signal and to calculate the proportionality parameter t for Eq.(7). It is obvious that for elastic scattering or for the simple straight beam echo experiment shown in Fig. 1, we get what we had before, namely: $\ell_1 H_1 = \ell_o H_o$, since $\bar{v}_1 = \bar{v}_o$.

It can be shown quite generally that the NSE conditions in Eqs.(10) or (11) describe the centre of the NSE group for a scattering process with energy change ω_o. The essential thing Eq.(7) implies is that φ depends only on the energy transfer ω, which is the relevant parameter for the sample scattering, and it does not explicitly depend on v_o and v_1 separately. Thus the NSE equation (7) is equivalent to the condition

$$\left(\frac{\partial \varphi}{\partial v_i}\right)_{\omega=\omega_o} = 0 \qquad (12)$$

which has just the form of Eq.(4), and it states that phase φ is stationary over the scattered beam, i.e. the neutrons having suffered an energy change ω_o in the scattering will produce much the same NSE signal as in Fig. 1, but centred at $\ell_1 H_1 / \ell_o H_o \neq 1$ [cf. Eq.(11)].

The sample scattering is characterized by the scattering function $S(\vec{\kappa},\omega)$, which will be assumed at this point to depend only on ω, since for the moment we are looking at the energy transfers only. This function describes the probability that the neutrons are scattered with the energy change ω, and thus it will give, via Eq.(7), the distribution function of φ's in the scattered beam. Consequently, the NSE signal

will be given as

$$P_{NSE} = P_S\langle\cos(\varphi-\bar{\varphi})\rangle = P_S\frac{\int S(\vec{\kappa},\omega)\cos[t(\omega-\omega_o)]d\omega}{\int S(\vec{\kappa},\omega)d\omega} \quad , \tag{13}$$

where P_S takes into account the eventual change of the neutron polarization by the scattering action itself which will be dealt with in detail in Section 4. If there is no spin scattering and high magnetic field involved, $P_S=1$. We have to remember, however, that the proportionality (7) between $\varphi-\bar{\varphi}$ and $\omega-\omega_o$, only holds to first order around $\bar{v}_o$ and $\bar{v}_1$, i.e. within a restricted range of δv_o and δv_1. Thus the integrations in Eq.(13) have to be restricted to this range, which means that in practice the incoming beam has to be roughly monochromatic and eventually an analyser has to be used for the outgoing beam, too. This amounts to using NSE in combination with a classical background spectrometer. This is a very general feature and, in addition to the ω resolution obtained by the spin echo, this background spectrometer provides the momentum $\vec{\kappa}$ resolution. Thus Eq.(13) shows that the NSE signal P_{NSE} corresponds to the ω Fourier transform of a given part of $S(\vec{\kappa},\omega)$ as singled out by the transmission function ("resolution ellipsoid" in the usual terminology) of the background spectrometer. This situation is illustrated in Fig. 4 where the shaded areas correspond to this transmission function, and it is also shown that by measuring only $\omega-\omega_o$ one can study quasi-elastic scattering problems ($\omega_o=0$) and optical-like, flat sections of elementary excitation branches ($\omega_o\neq0$). Experimental examples for both cases are described in various contributions to this volume.

In order to obtain full information about the scattering function in Eq.(13), P_{NSE} has to be measured at several values of the Fourier parameter t, i.e. at several values of H_o at constant H_o/H_1 [cf. Eqs.(11)]. For example, if the studied part of $S(\vec{\kappa},\omega)$ corresponds to a Lorentzian line, which is narrow compared with the background spectrometer transmission function (Fig. 4) and is centred at ω_o:

$$S(\vec{\kappa},\omega) \propto \frac{\gamma}{\gamma^2+(\omega-\omega_o)^2} \quad , \tag{14}$$

the integration in Eq.(13) can be taken from $-\infty$ to ∞, and it gives

$$P_{NSE}(t) = P_S\frac{\int_{-\infty}^{\infty}[\gamma^2+(\omega-\omega_o)^2]^{-1}\cos[t(\omega-\omega_o)]d\omega}{\int_{-\infty}^{\infty}[\gamma^2+(\omega-\omega_o)^2]^{-1}d\omega} = e^{-\gamma t} \quad . \tag{15}$$

Thus, from the t dependence of P_{NSE} one can check if the line is really Lorentzian and one can then determine the linewidth parameter γ.

In practice, the measurement of P_{NSE} occurs in two steps. First the spectrometer has to be calibrated by measuring the NSE signal for a standard sample with

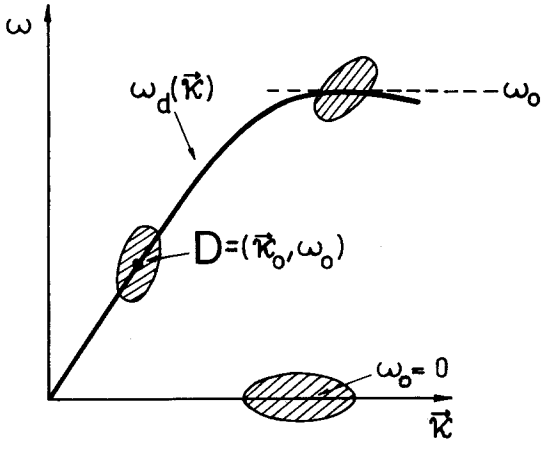

Fig. 4. The role of the transmission function of the host ("background") spectrometer in providing momentum resolution and selection of the scattering process in different types of NSE experiments.

$\gamma=0$ (e.g. elastic scatterer), and $P_S=1$, of course. The obtained $P^o_{NSE}(t)$ function can be considered as the instrumental resolution function since it differs from 1 due only to the finite overall polarization efficiency of the spectrometer and, what is more important, due to the residual dephasing of the Larmor precessions brought about by the inhomogeneities of the magnetic precession fields H_o and H_1. The absolute value of these inhomogeneities increases with increasing H_o and H_1, thus $P^o_{NSE}(t)$ itself depends strongly on t, as shown by the experimental curve in Fig. 5.

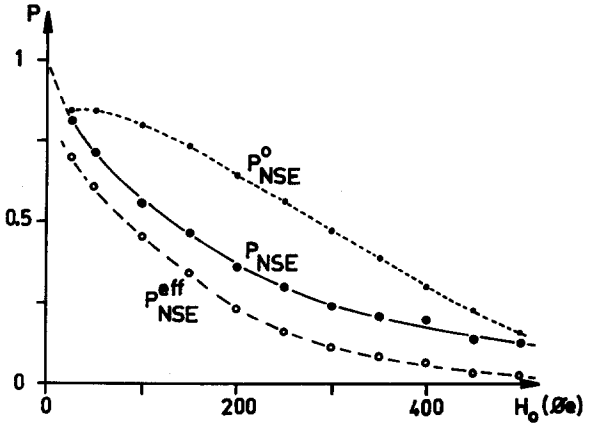

Fig. 5. An example for NSE spectrometer calibration and data reduction (see text). The corrected spectrun P_{NSE} corresponds to a quasielastic scattering line with 0.24 μeV half-width at half maximum. H_o is proportional to the time parameter t, cf. Eq. (11). (IN11 data)

This instrumental broadening of the φ distribution will then convolute with the one that corresponds to $S(\vec{\kappa},\omega)$ of the sample, which convolution will be translated by the Fourier transformation in Eq.(13) to multiplication, viz. the NSE signal P_{NSE}^{eff} directly observed for the sample will be given as

$$P_{NSE}^{eff}(t) = P_{NSE}(t) \cdot P_{NSE}^{o}(t) \quad , \tag{16}$$

where $P_{NSE}(t)$ is the function we have been considering above and the one we wish to obtain from the NSE experiment. Thus, in contrast to the usual methods, the instrumental resolution effects are taken into account by simple division instead of an often ambiguous and tedious deconvolution. This feature of NSE is fundamental for line-shape studies.

Let us note that for quasi-elastic scattering with $\omega_o=0$, $P_{NSE}(t)$ can be given a concrete interpretation. Since the scattering function of the sample $S(\vec{\kappa},\omega)$ is given as the Fourier transform of the space - time correlation function $S(\vec{r},t)$, the cosine Fourier transform in Eq.(13) will lead back to the so-called intermediate scattering function, viz.

$$P_{NSE}(t) = P_S \cdot \mathrm{Re}\ S(\vec{\kappa},t) \quad , \tag{17}$$

where t has the meaning of real, physical time. For isotropic systems $S(\vec{\kappa},t)$ is purely real, thus $P_{NSE}(t)$ is precisely the time dependent correlation function for fluctuations with the selected wave vector $\vec{\kappa}$.

Before turning to the more general formulation of the NSE method, let us consider the conceptual difference between NSE and conventional inelastic neutron scattering techniques. Conventionally, the energy transfer $\hbar\omega$ is measured by taking the difference of the outgoing and incoming energies, i.e. as a difference of two beam averages: $\frac{1}{2}m\langle v_1^2\rangle - \frac{1}{2}m\langle v_o^2\rangle$. The resolution in ω is thus limited by the scatter of both v_1 and v_o. In view of this, high resolution implies correspondingly good monochromatization, i.e. low neutron intensity, which relation comes directly from the well-known Liouville theorem. In NSE the beam average of $\cos\varphi$ is measured in a single step, i.e. of a quantity which is directly related to the energy change ω. Consequently, the ω resolution becomes independent of the incoming and outgoing beam monochromatization, and the Liouville relation between intensity and resolution does not apply. This feature and the high inherent sensitivity of the Larmor precession technique are the clues to the new possibilities offered by NSE in high resolution inelastic neutron scattering spectroscopy.

3. THE GENERAL PRINCIPLE OF NSE

In the previous section we dealt with scattering functions which locally depend only on ω and not on $\vec{\kappa}$. The NSE method in its most general form, as introduced in

Ref. 5, (see also the Appendix) can be applied to $\vec{\kappa}$ dependent processes too, like elementary excitations with a general dispersion relation (cf. Fig. 4). In Ref. 5 this generalization was obtained from the following basic idea. The scattering of a given neutron is described by the incoming and outgoing velocity or momentum vectors $\vec{\kappa}_o = \frac{m}{\hbar}\vec{v}_o$ and $\vec{\kappa}_1 = \frac{m}{\hbar}\vec{v}_1$, respectively. The sample scattering functions on the other hand depend on the transfer parameters

$$\vec{\kappa} = \frac{m}{\hbar}(\vec{v}_1 - \vec{v}_o)$$
$$\hbar\omega = \frac{1}{2}m(v_1^2 - v_o^2) \qquad (18)$$

(Note that throughout this paper the absolute value of a vector is denoted by its symbol without the arrow, i.e. $v_1 = |\vec{v}_1|$, etc.) Thus the four parameters $(\vec{\kappa},\omega)$ are the relevant ones, whereas in conventional neutron scattering spectroscopy the six irrelevant parameters $(\vec{v}_o,\vec{v}_1)$ are measured separately. The redundant 6-4=2 free parameters are at the origin of the complexity of the resolution calculations, and since $\vec{\kappa}$ and ω are both obtained as differences of separately measured quantities $\vec{\kappa}_o$ and $\vec{\kappa}_1$ [cf. Eqs.(18)], the Liouville relation between intensity and resolution applies and it alone sets the limits for resolution. (In the classical type backscattering method basically designed for $\vec{\kappa}$ independent scattering effects, very much intensity can be gained back by the use of huge detector solid angles, cf. the paper by A. Heidemann et al.) The quantity involved in general NSE experiments, the total Larmor precession angle φ - which most generally will be given as $\varphi=\varphi(\vec{v}_o,\vec{v}_1)$ - depends on both the incoming and the outgoing neutron parameters. It is then conceivable that this function φ has special symmetry in that it depends (locally) on only four relevant combinations (18) of six irrelevant parameters $(\vec{v}_o,\vec{v}_1)$. Thus for the local variation we require that $\varphi=\varphi(\vec{\kappa},\omega)$, that is,

$$\delta\varphi = \vec{\alpha}\delta\vec{\kappa} + \beta\delta\omega \quad , \qquad (19)$$

where $\vec{\alpha}$ and β are constants. This equation is the most general formulation of NSE. It implies that φ becomes locally, around a point in the $(\vec{\kappa},\omega)$ space, exactly the same kind of four parameter function as $S(\vec{\kappa},\omega)$, and thus, if properly matched, it can effectively probe $S(\vec{\kappa},\omega)$ directly in a single step measurement, and it is not affected by the Liouville intensity-resolution relation.

Here I will present a more obvious though less general reasoning which, however, leads to the same result. The aim of doing this is to give insight to the significance of the above argument, which in turn made sure that nothing gets omitted.

Let us consider how the fundamental NSE equation (7) could be generalized for the study of dispersive elementary excitation branches. What we have to know in such a case is the behaviour of $S(\vec{\kappa},\omega)$ as a function of the distance from the dispersion

relation $\omega_d(\vec{\kappa})$. Indeed, we expect that $S(\vec{\kappa},\omega)$ changes little along the $\omega_d(\vec{\kappa})$ surface, i.e. in going along the "ridge" of the excitation branch, but it changes rapidly when going across. This amounts to the assumption that locally, around the point $D=(\vec{\kappa}_o,\vec{\omega}_o)$ (cf. Fig. 4), the scattering function can be approximated by the single variable function S_D as

$$S(\vec{\kappa},\omega) = S_D[\omega-\omega_d(\vec{\kappa})] \tag{20}$$

Note that in effect $S(\vec{\kappa},\omega)$ as it appears in the experiment is already modified by the background spectrometer transmission function $T(\vec{\kappa},\omega)$. Thus, $S_D[\omega-\omega_d(\vec{\kappa})]$ actually corresponds to the behaviour of $S(\vec{\kappa},\omega)T(\vec{\kappa},\omega)$ averaged over the shaded area where $T(\vec{\kappa},\omega)\neq 0$.

If there are scattering contributions inside the transmission area other than the ω_d dispersion relation we are interested in, these will also be included in S_D but they will tend to give only a flat background below the peak at $\omega-\omega_d=0$.

In order to probe function S_D using the NSE Larmor precession angle φ, we require, instead of Eq.(7),

$$\varphi-\bar{\varphi}=t[\omega-\omega_d(\vec{\kappa})] \quad , \tag{21}$$

where $\vec{\kappa}=m(\vec{v}_1-\vec{v}_o)/\hbar$, furthermore $\varphi=\varphi(\vec{v}_o,\vec{v}_1)$, and $\bar{\varphi}=\varphi(\bar{\vec{v}}_o,\bar{\vec{v}}_1)$ with the average velocities $\bar{\vec{v}}_o$ and $\bar{\vec{v}}_1$ being assumed to correspond to the point D on the dispersion relation around which it is being looked at, that is,

$$\hbar\vec{\kappa}_o = m(\bar{\vec{v}}_1-\bar{\vec{v}}_o) \qquad \hbar\omega_o = \tfrac{1}{2}m(\bar{\vec{v}}_1^2-\bar{\vec{v}}_o^2)$$
$$\omega_d(\vec{\kappa}_o) = \omega_o \tag{22}$$

Equation (21) is the final, general NSE equation which can again be satisfied to first order in $\delta\vec{v}_i=\vec{v}_i-\bar{\vec{v}}_i$ $(i=0,1)$. Note that in order to tackle $\vec{\kappa}$ dependent scattering functions we have to consider the full vector-character of the incoming and outgoing neutron velocities, whereas above it was sufficient to look at their absolute values.

The right hand side of our fundamental equation (21) can, in view of Eqs.(22), be written in the differential form

$$\omega-\omega_d(\vec{\kappa}) \simeq \omega-[(\vec{\kappa}-\vec{\kappa}_o)\cdot\mathrm{grad}\omega_d(\vec{\kappa}_o)+\omega_d(\vec{\kappa}_o)] =$$
$$= \frac{m}{\hbar}(\bar{\vec{v}}_1-\mathrm{grad}\omega_d)\delta\vec{v}_1 - \frac{m}{\hbar}(\bar{\vec{v}}_o-\mathrm{grad}\omega_d)\delta\vec{v}_o \quad , \tag{23}$$

where $\mathrm{grad}\omega_d=(\frac{\partial\omega_d}{\partial\kappa_x}, \frac{\partial\omega_d}{\partial\kappa_y}, \frac{\partial\omega_d}{\partial\kappa_z})$.

It is seen that $\omega-\omega_d(\vec{\kappa})$ is a vectorial function of $\delta\vec{v}_i$'s, and obviously the matching $\varphi(\vec{v}_o,\vec{v}_1)$ function has to have the same character i.e. φ has to depend on the direction of v_i's too, not only on their absolute values as in Eq.(5). This can be achieved,

as suggested in Ref. 5 and shown in Fig. 6, by using precession field regions tilted with respect to the main beam directions $\vec{\bar{v}}_i$. (Another solution has already been tried out, and it is described in this volume in the report on ^{4}He excitations.)

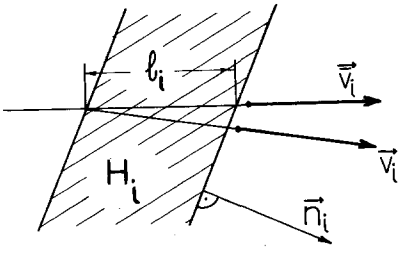

Fig. 6. Magnetic field configuration for producing Larmor precessions which depend on the direction of the neutron velocity.

It easy to see in Fig. 6 that the Larmor precession angles φ_i can be given in the differential form, [cf. Eq.(1)]:

$$\varphi_i(\vec{v}_i) = \gamma_L \frac{\ell_i H_i}{\bar{v}_i} - \gamma_L \frac{\ell_i H_i}{\bar{v}_i^2}(\vec{n}_i \delta\vec{v}_i) \quad , \tag{24}$$

where $\vec{n}_i$ is normalized so that $(\vec{n}_i \vec{\bar{v}}_i)=\bar{v}_i$. Thus the left hand side of the NSE equation (21) reads $[\bar{\varphi}_i=\varphi_i(\vec{\bar{v}}_i)]$

$$\varphi-\bar{\varphi} = (\varphi_o-\bar{\varphi}_o)-(\varphi_1-\bar{\varphi}_1) = -\gamma_L \frac{\ell_o H_o}{\bar{v}_1^2}(\vec{n}_o \delta\vec{v}_o)+\gamma_L \frac{\ell_1 H_1}{\bar{v}_1^2}(\vec{n}_1 \delta\vec{v}_1) \quad . \tag{25}$$

Equation (21) is satisfied if and only if the vector coefficients of the $\delta\vec{v}_i$'s agree on both sides, i.e. by Eqs.(23) and (25) (i=0,1)

$$\gamma_L \frac{\ell_i H_i}{\bar{v}_i^2}\vec{n}_i = t\frac{m}{\hbar}[\vec{\bar{v}}_i - \mathrm{grad}\omega_d(\vec{\kappa}_o)] \quad . \tag{26}$$

This equation immediately defines the direction of the vectors $\vec{n}_i$, i.e. the field tilt angles ϑ_i contained by $\vec{n}_i$ and $\vec{\bar{v}}_i$:

$$\vec{n}_i \,||\, [\vec{\bar{v}}_i - \mathrm{grad}\omega_d] \quad , \tag{27}$$

and by multiplying both sides of Eq.(25) with $\vec{v}_i$, we get

$$\gamma_L \frac{\ell_i H_i}{\bar{v}_i} = t\frac{m}{\hbar}[\bar{v}_i^2 - (\vec{v}_i \cdot \mathrm{grad}\omega_d)] \quad ,$$

which for convenience can be rewritten (with $\bar{E}_i = \frac{1}{2}m\bar{v}_i^2$) as

$$\frac{\ell_o H_o}{\ell_1 H_1} = \frac{\bar{v}_o^3 - \bar{v}_o(\vec{v}_o \cdot \mathrm{grad}\omega_d)}{\bar{v}_1^3 - \bar{v}_1(\vec{v}_1 \cdot \mathrm{grad}\omega_d)} \quad , \tag{28}$$

$$t = \hbar \frac{\gamma_L \ell_i H_i}{\bar{v}_i m(\bar{v}_i^2 - \vec{v}_i \cdot \mathrm{grad}\omega_d)} = \hbar \frac{\bar{\varphi}_i}{2\bar{E}_i - m(\vec{v}_i \cdot \mathrm{grad}\omega_d)} \quad . \tag{29}$$

Equations (28) and (29) determine the ratio of the precession field strengths and the time-like constant t in Eq.(21). It will be shown later how t is related to the real, physical time.

The distribution of $\omega - \omega_d(\vec{\kappa})$ for the investigated scattering process being given by the S_D function [cf. Eq.(20)], by virtue of Eq.(21) one gets for the NSE signal

$$P_{NSE}(t) = P_S \frac{\int_{-\infty}^{\infty} S_D(\omega)\cos(t\omega)\,d\omega}{\int_{-\infty}^{\infty} S_D(\omega)\,d\omega} \quad . \tag{30}$$

Note that since S_D is a single parameter function vanishing outside the width of the transmission function T, in Eq.(30) ω is just the energy integration parameter. In the experiment, as already discussed above, $P_{NSE}(t)$ will be measured using the normalization to the instrumental effects contained in $P^o_{NSE}(t)$, and S_D can then be obtained by Fourier transformation if necessary.

The setting up of the NSE experiment for the study of a given excitation consists of tuning the NSE parameters: $\vec{n}_o$, $\vec{n}_1$ (i.e. ϑ_o, ϑ_1) and H_o/H_1 to the values given by Eqs.(27) and (28). It can be seen that these depend not only on $(\vec{\kappa}_o, \omega_o)$ via $\vec{v}_o$ and $\vec{v}_1$, but also on the slope of the dispersion relation $\mathrm{grad}\omega_d(\vec{\kappa}_o)$. This special feature of NSE can be useful in selecting out a given excitation branch at points where branches overlap or hybridize. Obviously for the special case $\mathrm{grad}\omega_d = 0$ this general formulation reduces to what we have seen in the previous section.

The transmission areas in Fig. 4, as pointed out above, are defined by the background spectrometer with which the NSE setup is combined. For the study of elementary excitations, where a reasonable $\vec{\kappa}$ resolution is required (few %), the most obvious choice for the background spectrometer is the triple axis spectrometer. This particular combination is discussed in detail by Roger Pynn later in this book, and in the Appendix[6].

Let us keep in mind that all the conditions for matching the NSE to a particular elementary excitation have been shown to be satisfiable to first order only. Higher

order terms will introduce instrumental resolution limitations, especially since in many cases they will not be directly measureable but only calculable, similarly to usual spectrometer resolution functions. To assess their importance we performed Monte Carlo simulation calculations with Laci Mihâly[7], which have shown that this fundamental limitation is typically not worse than 1-5 μeV for usual phonons and magnons. This is illustrated in Fig. 7 by the sample simulation result obtained for an NSE-triple axis configuration with typical collimations and monochromator-analyser mosaicities. It is seen that the distribution of $\varphi-\bar{\varphi}$, the $p(\varphi-\bar{\varphi})$ function (dots and dashed lines) reproduces with minimal (~2 μeV) broadening the distribution of $\omega-\omega_d(\vec{\kappa})$, which for the assumed three parallel phonon branches (insert to Fig. 7) corresponds to an S_D function consisting of three δ-functions separated from each other by only 20 μeV.

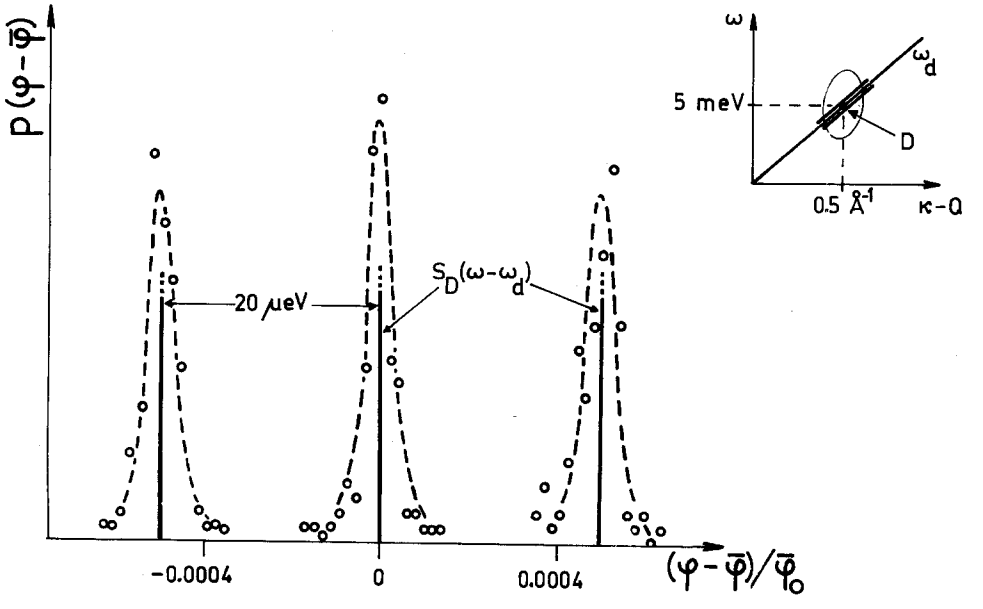

Fig. 7. Distribution of the total Larmor precession angle showing the general NSE focussing effect for inelastic scattering on dispersive elementary excitations (see text). The open circles are the data points calculated by Monte-Carlo simulation method, the dashed lines are guides to the eye. The vertical lines represent the $\omega-\omega_d$ energy distribution for the model longitudinal phonon branches with zero linewidth (see insert). The parameters of the assumed host triple-axis spectrometer configuration are: 2.5 Å incoming neutron wavelength; 40' graphite monochromator and analyser; energy loss scattering; Q=3 $Å^{-1}$ reciprocal lattice vector; 30'x30'x30'x30' collimation.

4. EFFECT OF SAMPLE SCATTERING

In this section we will consider the direct effect of the sample scattering process on the neutron spin polarization which is taken into account by the factor P_S [cf. Eq.(12)]. As mentioned above $P_S=1$ if we investigate non-magnetic scattering effects and, in addition, there is but a small magnetic field on the sample. This latter condition is essential because the various possible neutron paths in the sample differ considerably in length. Thus there is always a spurious dephasing of the Larmor precession angles, which is of the order of $\Delta\varphi=2\gamma_L H_s d\cdot\sin\frac{\vartheta}{2}/v$ where H_s is the magnetic field at the sample, d the relevant dimension of the sample, ϑ the scattering angle, and v the neutron velocity (Fig. 8). As is discussed in the paper by

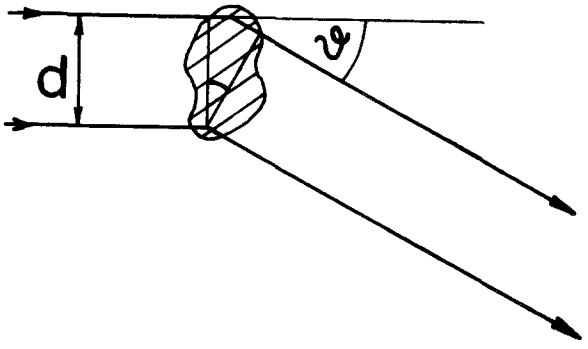

Fig. 8. Neutron path length differences in scattering on extended samples.

Otto Schärpf, some minimum guiding magnetic field is always required at the sample, so H_s cannot be arbitrarily small. For example, for $H_s=0.5$ Øe we get for a typical maximum sample size d=3 cm and $\lambda=5$ Å neutron wavelength $\Delta\varphi = 40^o\cdot\sin\frac{\vartheta}{2}$, which means just half of this amount as deviation from the average value of $\bar{\varphi}$. Table I below shows the effect of dephasing on the precessing polarization, assuming uniform distribution of precession angles between $\bar{\varphi}-\frac{1}{2}\Delta\varphi$ and $\bar{\varphi}+\frac{1}{2}\Delta\varphi$. It is seen that H_s fields of the order of 0.5 Øe, already sufficient as guide fields, produce negligible polarization losses. On the other hand fields with values of H_s greater than 5 Øe destroy the echo for large samples and scattering angles above 90°, and for higher fields this limiting scattering angle decreases. Strong H_s fields of the order of 1 kØe and above at the sample would therefore be excluded by this effect alone and, in addition, such high fields inevitably display considerable inhomogeneities too. (However, by the use of a trick which will be introduced below as the Ferromagnetic Neutron Spin Echo, this difficulty can be circumvented at the expense of a 50 % reduction of the echo signal.) At this point we conclude that in ordinary NSE the field at the sample has to be kept at a low value, which depends on the geometry of the experiment. This condition, usually corresponding to an upper limit of few Øe, is generally easily met.

Table I.

Reduction factor η for the precessing polarization produced by uniform distribution of precession angle differences between 0 and $\Delta\varphi$

$\Delta\varphi$	η	$\Delta\varphi$	η
20^o	0.995	180^o	0.637
40^o	0.980	200^o	0.564
60^o	0.955	220^o	0.489
80^o	0.921	240^o	0.413
100^o	0.878	260^o	0.338
120^o	0.827	280^o	0.263
140^o	0.769	300^o	0.191
160^o	0.705	320^o	0.121

It is interesting to observe that the very reason that NSE, an essentially time--of-flight method, can be of very high resolution is that it is not simply the path lengths that count here, but those weighted by the magnetic field values $S_L=\int Hds$. Thus, a high precision of the flight path definition is only required for the precession field regions H_o and H_1 (where it means stringent requirements, equivalent to better than 0.1 mm geometrical precision, which is to be met by the homogeneity of the fields), whereas differences of several centimetres can be tolerated in the low field regions, viz. at the sample, where, for high scattering angles, these differences are bound to be comparable to the sample dimensions.

In order to study the effect of magnetic sample scattering, we need to have a look at the action of the spin flipper device separating the two precession fields H_o and H_1 near to the sample (Fig. 9). As mentioned above, in practice the opposite sign of the φ_o and φ_1 precessions is produced by this device, also known as a π-coil, and not by a theoretically equivalent 180^o flip of the field direction between H_o and H_1. This point will be discussed at length in the next contribution, here we merely anticipate part of it. If we consider the spin precession plane (x,y) we can envisage the flipper action as a 180^o turn of the neutron spin around an arbitrary axis in this plane, e.g. around the x axis. Thus a neutron spin polarization $\vec{P}=(P_x,P_y,P_z)$ will be flipped into $\vec{P}'=(P_x,-P_y,-P_z)$. The precession angle φ_o, measured for convenience with respect to the x axis (Fig. 9a) and given as $\varphi_o=\arctan(P_y/P_x)$, will correspondingly be transformed in $\varphi_o'=\arctan(-P_y/P_x)=-\varphi_o$. This is precisely the key action to the echo: neutrons arriving at the π-coil with a precession angle φ_o, will appear to leave it with $-\varphi_o$.

At this point, if not earlier, the reader will probably ask himself a question about the significance of an obviously arbitrary $\pm 2\pi n$ (n=integer) term which can be added at any point to the phase φ. The question is completely justifiable and in

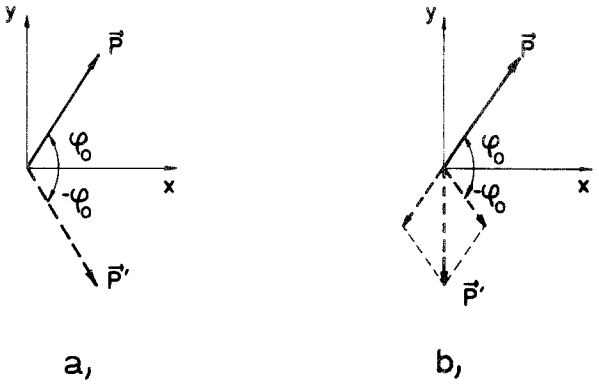

Fig. 9. Inversion of the sign of the Larmor precession angle by the application of a π spin flip coil (a) and in paramagnetic scattering (b).

effect this phase ambiguity drops out only as a consequence of a very natural assumption about the f(v) velocity distribution function, which was not mentioned before. This assumption is that f(v) is not too narrow, or has no too sharp structures so that after having gone through the first precession field H_o, the precessing polarization is completely dephased $\langle\exp(i\varphi_o)\rangle=\int f(v)\exp[i\varphi_o(v)]dv=0$. In this case the $\partial\varphi/\partial v=0$ sufficient echo condition, obviously unaffected by an extra $\pm 2\pi n$ term, becomes a necessary one, and no precessing polarization can be found outside the neutron spin echo group. To see a conspicuous example to the contrary, imagine that $f(v)=\delta(v-v_A)+\delta(v-v_B)$, with v_A and v_B being constants. In this case precessing polarization could occur around any values of H_o and H_1, due to the beating between the two velocity components v_A and v_B, and subsequent beating maxima would indeed be separated by a 2π phase difference. The NSE polarization signal measured at the values of the NSE parameters as given by Eqs.(11) or (28) above, will obviously be correct, i.e. correspond to the scattering function as required by Eqs.(13) or (30). But by inspection of the spectrometer response alone we would not be able to find out which of the beating maxima is the right NSE group. In practice such problems can occur only when the incoming beam is too monochromatic with respect to the number of Larmor precessions, that is $\langle\exp(i\varphi_o)\rangle\neq 0$. This corresponds to the illogical situation in which the NSE ω resolution is not really better than that of the background spectrometer. In such a case the maximum of the NSE group might not correspond to the ideal NSE conditions, examples for which are shown in Roger Pynn's article in this volume. Normally such a situation does not arise if NSE is used as it should be, i.e. to improve the ω resolution of the background configuration.

In what follows we will consider how NSE can work for various magnetic sample scattering processes in which the neutron spin direction changes. This change can be checked by simple neutron spin polarization analysis, without the echo. Its effect on the echo will be twofold: on the one hand it calls for an appropriate spin flipping scheme at the sample, and on the other, it gives rise to NSE sample scattering polarization factors P_S [introduced in connection with Eq.(13)] which are less than unity. Note that if there are several scattering processes contributing to the echo signal, the NSE spectrum $P_{NSE}(t)$ will be given by the weighted average. The knowledge of the different polarization behaviours of the different components might be helpful in their decomposition.

4.1 NSE with nuclear spin incoherent scattering

This process is characterized by the $\vec{P}' = -\frac{1}{3}\vec{P}$ equation, which relates the polarization $\vec{P}$ of the beam impinging on the sample with that of the scattered one $\vec{P}'$. Thus, in addition, to the slow Larmor precessions in the H_s field at the sample there is a $\varphi_o' = \varphi_o + \pi$ transformation of the precession angle. This, having no effect on $\partial\varphi/\partial v$, the echo signal appears at the same position, but with opposite sense (minima instead of maxima) and with amplitude reduced to $\frac{1}{3}$. Of course, the π-coil is necessary to produce the negative sign, and the total transformation between H_o and H_1 reads as $\varphi_o' = -\varphi_o \pm \pi$ (the sign of π being immaterial). This process obviously corresponds to $P_S = -\frac{1}{3}$.

4.2 Paramagnetic Neutron Spin Echo[8] (PNSE)

Paramagnetic scattering, which can be defined most generally as scattering on a macroscopically isotropic magnetic sample (i.e. with no strong magnetic field H_s and with isotropically distributed orientations for any kind of eventual locally ordered domains), is characterized by the relation

$$\vec{P}' = -\vec{\kappa}(\vec{P}\cdot\vec{\kappa})/\kappa^2 \qquad (31)$$

between the incoming and scattered beam polarization. This polarization behaviour is well-known for the scattering on spin paramagnets, but it will be shown in Sub-section 4.4 below, that it is valid more generally for isotropic magnetic systems with both orbital and spin magnetism.

It is clear from Eq.(31) that if $H_s \| \vec{\kappa}$, i.e. the precession plane (x,y) is perpendicular to $\vec{\kappa}$, $\vec{P}'$ will be 0 for any $\vec{P}$ in this plane, and thus no spin echo can occur in this geometry. We will therefore assume that the $\vec{\kappa}$ scattering vector lies in the precession plane and, for convenience, its direction will be taken as the y axis with φ_o measured with respect to the x axis. (If $\vec{\kappa}$ is at an angle Θ with respect to the (x,y) plane, its projection is the y axis, and the final polarization will be reduced by a factor of $\cos\Theta$). Equation (31) then corresponds to the transformation:

$$\vec{P}' = (0,-P_y,0) = (\tfrac{1}{2}P_x,-\tfrac{1}{2}P_x,0)+(-\tfrac{1}{2}P_x,-\tfrac{1}{2}P_y,0) \qquad (32)$$

The first term on the right hand side corresponds to the $\varphi_o' = -\varphi_o$ flip; the second to

$\varphi_o'=\varphi_o+\pi$. Thus without any further π-coil action the first term with the key negative sign for φ_o will give an echo signal of an amplitude reduced by $\frac{1}{2}$, that is, $P_S=\frac{1}{2}$ (cf. Fig. 9b) or if we use a flipper at the sample, an echo signal of similar amplitude but opposite phase will be observed, due to the second term ($P_S=-\frac{1}{2}$), just as for case 4.1. The first possibility is of particular importance since without a flipper there will be no confusing contributions to the echo from non-magnetic or nuclear spin scattering effects.

In order to be able to normalize the PNSE signal, we have to know the denominator in Eq.(13), viz. the total paramagnetic scattering intensity separated from the other contributions. This can easily be achieved by the following, novel procedure[8]. Let us take classical polarization analysis "spin up" (no-spin-flip) and "spin down" (spin-flip) counts, with H_s parallel to the x direction of a coordinate system, and repeat this with $H_s||y$ and $H_s||z$. Since in this case $\vec{P}||H_s$ to start with, and $\vec{P}'$ is also analysed parallel to $H_s||\vec{P}$, the paramagnetic contribution to the $N_\uparrow-N_\downarrow$ counting rate modulation is given as [cf. Eq.(32)]

$$N_\uparrow^P-N_\downarrow^P = N_P(\vec{P}\cdot\vec{P}') = -N_P(\vec{P}\cdot\vec{\kappa})^2/\kappa^2 \quad , \tag{33}$$

where N_P is the total paramagnetic intensity we want to determine. Adding together the modulations for the three subsequent $\vec{H}_s$ orientations, x, y and z, we get

$$\sum_{j=x,y,z}(N_\uparrow^P-N_\downarrow^P)_j = -N_P|\vec{P}|^2(\kappa_x^2+\kappa_y^2+\kappa_z^2)/\kappa^2 = -N_PP^2 \quad , \tag{34}$$

where in effect P^2 stands for the efficiency of the polarizer-flipper-analyser system. In addition we make sure that one of the axes, say the y axis, is perpendicular to $\vec{\kappa}$ (e.g. by being perpendicular to the scattering plane) in which case we get $\kappa_y=0$, i.e. the paramagnetic modulation $(N_\uparrow^P-N_\downarrow^P)_y=0$, and we can observe the pure contribution of the non-paramagnetic (NP) effects, for which $\vec{P}'=\vec{P}$ always holds:

$$(N_\uparrow^{NP}-N_\downarrow^{NP})_y=N_{NP}P^2 \quad . \tag{35}$$

Since this contribution is the same for x and z, we find for the combination below of the total modulations with $N=N^P+N^{NP}$,

$$\sum_{j=x,y,z}(N_\uparrow-N_\downarrow)_j-3(N_\uparrow-N_\downarrow)_y=(N_\uparrow-N_\downarrow)_x+(N_\uparrow-N_\downarrow)_z-2(N_\uparrow-N_\downarrow)_y=-N_PP^2 \tag{36}$$

An example of PNSE experiment is described in the contribution of Amir Murani and in Ref. 8 (see the Appendix).

4.3 Ferromagnetic Neutron Spin Echo (FNSE)

If we wish to study a ferromagnetic sample by NSE, we have to apply a strong magnetic field to saturate it, in order to avoid the well-known complete depolarization of the beam. Thus, as pointed out above, the Larmor precession will be completely dephased around the sample, and all information contained in φ_o's concerning the incoming beam polarization are lost, unless we do something about it. The situation

is obviously the same for all samples which have to be studied in a "high" magnetic field, independently of ferromagnetism.

We will utilize the simple fact that the non-precessing $z||H_s$ component of the polarization is maintained in a proper adiabatic guide field, as it is well-known in polarized neutron work. Thus, applying a 90^o turn to the neutron spins after H_o, we can turn one component of the (x,y) precessing polarization, say x, into the z direction. This can then be turned back by another $\frac{\pi}{2}$ coil to the relevant x direction after the scattering, when entering H_1. The other two components are assumed to be completely dephased in the sample region, i.e. the spin history between H_o and H_1 is the following

$$(P_x,P_y,P_z) \rightarrow (P_z,-P_y,P_x) \rightarrow (0,0,P_x) \rightarrow (P_x,0,0)$$

$$\uparrow \tfrac{\pi}{2}\ \text{coil} \qquad \uparrow H_s\ \text{field} \qquad \uparrow \tfrac{\pi}{2}\ \text{coil}$$

The final polarization $\vec{P}'=(P_x,0,0)$ can be considered again as a sum of two terms

$$(P_x,0,0) = (\tfrac{1}{2}P_x,\tfrac{1}{2}P_y,0)+(\tfrac{1}{2}P_x,-\tfrac{1}{2}P_y,0) \quad , \qquad (37)$$

where the first corresponds to $\varphi_o'=\varphi_o$ and the second to $\varphi_o'=-\varphi_o$. Thus the second term gives an echo signal of 50 % amplitude ($P_S=\frac{1}{2}$).

Note that here the complete elimination of P_y, a necessary condition for FNSE to work correctly, corresponds to "forgetting" the sense of the rotation for φ_o, i.e. mathematically it corresponds to going from $e^{i\varphi_o}$ to $\cos\varphi_o=\frac{1}{2}e^{i\varphi_o}+\frac{1}{2}e^{-i\varphi_o}$. This method has been tested but not yet used in experiments. Its applications can include, besides experiments in high fields, in particular the study of magnons for which an additional spin-flip occurs at the scattering, $P_x' \rightarrow -P_x$, which produces a change in the sign of the echo signal described by $P_S=-\frac{1}{2}$.

4.4 Antiferromagnetic Neutron Spin Echo (AFNSE)

In the previous section we have seen that the introduction of a preferred magnetization direction in a ferromagnet necessarily leads to the primary dephasing of the Larmor precessions around the sample, due to the saturation moment and the high magnetizing field. On the other hand, in an antiferromagnetic single crystal the crystalline symmetry might produce a preferred direction, or a few preferred directions for the atomic magnetic moments, without any strong field to be applied. We will therefore consider NSE experiments on magnetically anisotropic samples in low magnetic fields. The cardinal point is that the polarization behaviour of the neutron beam scattered from a macroscopically isotropic magnetic sample is exactly the same as for paramagnetic samples, i.e. $\vec{P}'=-\vec{\kappa}(\vec{P}\cdot\vec{\kappa})/\kappa^2$. (Because this theorem does not seem to have been recognized before, it will be proved below.) Thus the paramagnetic NSE situation will apply to any sample, paramagnetic or not, in which the eventual local anisotropies (e.g. preferred direction of the moments) are averaged out on the macroscopic scale. Similarly, the antiferromagnetic NSE will be defined as the situation

that applies to samples with zero saturation moment and with macroscopically anisotropic magnetic correlations, even if they are not actually antiferromagnetic; an example of such a material would be a tetragonal single crystal displaying critical fluctuations in the paramagnetic phase.

Let us recall here that magnetic neutron scattering is related to the magnetization-magnetization correlation functions, which include both spin and orbital contributions[9]. For an isotropic system we have (i,j=x,y,z)

$$\begin{aligned} &\langle M_i \rangle = 0 \\ &\langle M_i^* M_j \rangle = 0 \quad i \neq j \\ &\langle M_i^* M_i \rangle = \langle M_j^* M_j \rangle \end{aligned} \tag{38}$$

The first two lines follow from the fact that the symmetry operation of 180° rotation, e.g. around the y axis, would transform M_x to $M_{-x}=-M_x$ and $\langle M_x M_y \rangle$ to $\langle M_{-x} M_y \rangle$.

Identifying the $\vec{\alpha}$ interaction potential in equations (10.37) and (10.41) on pp. 330 and 331 of Ref. 9 with the component of the magnetization vector perpendicular to the momentum transfer $\vec{\kappa}$, viz.

$$\vec{M}_\perp(\vec{\kappa}) = \vec{M}(\vec{\kappa}) - \vec{\kappa}[\vec{M}(\vec{\kappa})\cdot\vec{\kappa}]/\kappa^2 \quad ,$$

we are left with the following very general expression, after suppression of the terms vanishing by virtue of Eqs.(38), for the scattered beam polarization:

$$\vec{P}' = \frac{\langle \vec{M}_\perp^*(\vec{M}_\perp\vec{P})\rangle + \langle(\vec{M}_\perp^*\vec{P})\vec{M}_\perp\rangle - \vec{P}\langle(\vec{M}_\perp^*\vec{M}_\perp)\rangle}{\langle(\vec{M}_\perp^*\vec{M}_\perp)\rangle} \quad , \tag{39}$$

where the < > brakets stand for the averaging over the sample states as given in detail in equation (10.33) in Ref. 9. For clarity and simplicity we will consider this equation in a coordinate system for which $\vec{\kappa}/\kappa$ is one of the base unit vectors, say $\vec{x}$. Thus $\vec{M}_\perp=(0,M_y,M_z)$ and

$$\begin{aligned} \vec{P}' &= \frac{\langle \vec{M}_\perp^*(P_y M_y + P_z M_z)\rangle + \langle(P_y M_y^* + P_z M_z^*)\vec{M}_\perp\rangle}{\langle M_y^* M_y + M_z^* M_z\rangle} - \vec{P} = \\ &= \frac{2\vec{y}P_y\langle M_y^* M_y\rangle + 2\vec{z}P_y\langle M_z^* M_z\rangle}{\langle M_y^* M_y + M_z^* M_z\rangle} - \vec{P} \quad . \end{aligned} \tag{40}$$

In view of the last of the equations (38), finally we get

$$\vec{P}' = (0,P_y,P_z) - \vec{P} = -\vec{x}\cdot P_x = -\vec{\kappa}(\vec{P}\cdot\vec{\kappa})/\kappa^2 \quad , \tag{41}$$

which is the required result.

Note that the premises we used, i.e. Eqs.(38), mean somewhat less than total isotropy; they will be satisfied, for example, by a cubic single crystal too if it

contains equal volume fractions of opposite antiphase domains (if they apply), which is the condition for the first two equations in (38) to hold.

The simplest case of antiferromagnetic NSE is the example of a tetragonal single crystal with $0 \neq \langle M^*_y M_y \rangle - \langle M^*_z M_z \rangle = \langle M^*_y M_y + M^*_z M_z \rangle A$, where A describes the anisotropy, and there is no antiphase domain asymmetry. Thus from Eq.(40) we readily find that

$$\vec{P}' = (-P_x, AP_y, -AP_z) \quad .$$

If the sample guide field H_s is in the z direction we get for the precessing polarization, if (x,y) is the precession plane [P_z=0, cf. Eq.(32)]

$$\vec{P}' = \frac{1+A}{2}(-P_x, P_y) + \frac{1-A}{2}(-P_x, -P_y) \quad , \qquad (42)$$

where the first term shows the familiar $\varphi_o \rightarrow -\varphi_o$ flip, producing an NSE signal with the amplitude $P_S = \frac{1+A}{2}$. (The paramagnetic case corresponds to A=0.) The anisotropy also makes P_S depend on the crystal orientation, showing a maximum when the preferred magnetization direction is parallel to the y axis. For a tetragonal collinear antiferromagnet this maximum is unity which was in fact observed in an early test in 1974.

Finally, if the sample contains only a single AF antiphase domain, which is often difficult to achieve anyway, none of the above trivial symmetry arguments holds, and one has to go through the whole complicated formalism of polarization analysis in order to interpret the NSE results. This is the most specific case of AFNSE but, unfortunately, nothing simple and general can be said about it.

The main conclusions in this section are summarized in Table II below, which gives a list of the sample environments and the NSE signal amplitudes for the different types of echoes considered

Table II.

Different types of NSE configurations

Type	Sample environment: flipper coils	H_s field	NSE signal P_S
Normal NSE			
non-magnetic scattering	π	small	1
nuclear spin incoherent scattering	π	small	$-\frac{1}{3}$
Paramagnetic NSE (isotropic samples)	none	small	$\frac{1}{2}$
Ferromagnetic NSE	$\frac{\pi}{2} - \frac{\pi}{2}$	high	$\frac{1}{2}$
Antiferromagnetic NSE (anisotropic samples)	none	small	$\frac{1}{2} < P_S^{max} \leq 1$

Conclusion

We have seen that the NSE technique can be applied for a variety of inelastic scattering processes and for both magnetic or non-magnetic samples. But the real conclusion of this introductory paper is in fact contained in the contributions which follow. At this point I should just like to express my gratitude for many stimulating discussions to a large number of colleagues, first of all to the authors of this volume and to many others at the ILL together with those I have already thanked in the preface. I should particularly like to thank the audiences who attended the talks I have given at various places, whose questions and sometimes difficulties with these ideas were certainly invaluable for my own understanding.

REFERENCES

(1) G.M. Drabkin, E.I. Zabidarov, Ya.A. Kasman, and A.I. Okorokov, Zh'ETF 56, 478 (1969); Sov. Phys. JETP, 29, 261 (1969)

(2) F. Mezei, Z. Physik 255, 146 (1972)

(3) F. Mezei, in "Imaging Processes and Coherence in Physics", edited by M. Schlenker et al. (Lecture Notes Series, Springer Verlag, Heidelberg, 1980) p. 282

(4) J.B. Hayter and J. Penfold, Z. Physik B 35, 199 (1979)

(5) F. Mezei, in Neutron Inelastic Scattering 1977 (IAEA, Vienna, 1978) p. 125

(6) R. Pynn, J. Phys. E 11, 1133 (1978)

(7) L. Mihály, Thesis, Central Research Institute of Physics, Budapest, (1977) unpublished

(8) F. Mezei, and A.P. Murani, Proc. Neutron Scattering Conf., Jülich, August 1979, J. Mag. Mag. Mat. 14, 211 (1979)

(9) W. Marshall, and S.W. Lovesey, Theory of Thermal Neutron Scattering (Clarendon Press, Oxford, 1971)